



**Digital Commons@**

Loyola Marymount University  
LMU Loyola Law School

---

Physics Faculty Works

Frank R. Seaver College of Science and  
Engineering

---

3-1996

## A statistical study of transient events in the outer dayside magnetosphere

Jeff Sanny

*Loyola Marymount University, jeff.sanny@lmu.edu*

D. G. Sibeck

*Johns Hopkins University*

C. C. Venturini

*Loyola Marymount University*

C. T. Russell

*University of California, Los Angeles*

Follow this and additional works at: [https://digitalcommons.lmu.edu/phys\\_fac](https://digitalcommons.lmu.edu/phys_fac)



Part of the [Physics Commons](#)

---

### Digital Commons @ LMU & LLS Citation

Sanny, Jeff; Sibeck, D. G.; Venturini, C. C.; and Russell, C. T., "A statistical study of transient events in the outer dayside magnetosphere" (1996). *Physics Faculty Works*. 34.

[https://digitalcommons.lmu.edu/phys\\_fac/34](https://digitalcommons.lmu.edu/phys_fac/34)

This Article is brought to you for free and open access by the Frank R. Seaver College of Science and Engineering at Digital Commons @ Loyola Marymount University and Loyola Law School. It has been accepted for inclusion in Physics Faculty Works by an authorized administrator of Digital Commons@Loyola Marymount University and Loyola Law School. For more information, please contact [digitalcommons@lmu.edu](mailto:digitalcommons@lmu.edu).

## A statistical study of transient events in the outer dayside magnetosphere

J. Sanny,<sup>1</sup> D. G. Sibeck,<sup>2</sup> C. C. Venturini,<sup>1</sup> and C. T. Russell<sup>3</sup>

**Abstract.** The AMPTE CCE satellite frequently observed transient ( $1 \leq \tau \leq 8$  min) events marked by magnetic field strength increases and bipolar magnetic field signatures (peak-to-peak amplitudes  $\geq 4$  nT) while in the outer dayside magnetosphere. We report a survey of 59 prominent events observed from August to November 1984. The bipolar signatures and minimum variance analysis reveal that most events move poleward and antisunward, except in the immediate vicinity of local noon. Here the motion of the events appears to be better governed by the spiral/orthospiral interplanetary magnetic field (IMF) orientation than magnetic curvature forces associated with IMF  $B_y$ . The IMF orientation appears to have little or no influence on event occurrence or orientation. We interpret the events in terms of solar wind/foreshock pressure pulse induced ripples on the magnetopause surface. Our results can be reconciled with those obtained in previous studies which made use of ISEE 1/2, AMPTE IRM, and AMPTE UKS observations if pressure pulses produce large-amplitude events and bursty merging (or reconnection) produces small-amplitude events.

### Introduction

Russell and Elphic [1978] used ISEE 1/2 observations in the immediate vicinity of the dayside magnetopause to identify a number of transient (~1 min) events marked by enhanced magnetic field strengths and bipolar signatures in the magnetic field component normal to the nominal magnetopause. They termed events with these features flux transfer events (FTEs). Subsequent work showed that on average FTEs recur each 7 min just inside the dayside magnetopause during periods of southward interplanetary magnetic field (IMF) orientation but are generally absent during periods of northward IMF orientation [Rijnbeek *et al.*, 1984]. Event amplitudes decrease with distance inward from the magnetopause [Kawano *et al.*, 1992], pointing to an explanation in terms of processes occurring at the magnetopause.

There are several possible causes for the events, including impulsive penetration of solar wind plasma filaments [Lemaire, 1977], bursty merging (or reconnection) resulting in the formation of magnetic flux ropes or bubbles [Russell and Elphic, 1978], the Kelvin-Helmholtz instability [Southwood, 1979], and solar wind/foreshock pressure pulse driven magnetopause motion [Sibeck *et al.*, 1989a]. Although the impulsive penetration and Kelvin-Helmholtz instability models make several testable predictions, they are rarely invoked to explain transient events observed at the magnetopause.

In contrast, the bursty merging and pressure pulse mechanisms have been developed to the point where they make a full panoply of predictions concerning the characteristics of indi-

vidual events and their statistical occurrence patterns (see review by Sibeck [1994]). Distinguishing between these two mechanisms is important. Under the merging interpretation, the prevalence of transient events implies that bursty merging is a major contributor to the solar wind-magnetosphere interaction [e.g., Cowley, 1982]. Under the pressure pulse interpretation, the prevalence of transient events implies that the magnetosphere is constantly being buffeted by highly variable solar wind parameters, perhaps with preconditioning in the foreshock [Sibeck, 1990].

Since the bursty merging and pressure pulse models predict differing patterns for event occurrence, orientation, and direction of motion as a function of IMF orientation, local time, and latitude, statistical studies should help determine the relative significance of each model in the production of transient events. We begin by outlining the contrasting predictions of the two models concerning event occurrence patterns as a function of IMF orientation. We then present a case study and a statistical survey of transient events observed by the AMPTE CCE satellite in the outer dayside magnetosphere, and conclude with an attempt to reconcile the new results with those obtained in previous studies.

### Predictions of the Bursty Merging Model

Merging occurs when any one of several current layer instabilities [e.g., Schindler, 1974; Huba *et al.*, 1977; Lui *et al.*, 1991] enhances resistivities, disrupts currents, and allows magnetosheath and magnetospheric magnetic field lines to interconnect across the magnetopause. Since instability growth rates increase with increasing current density and there is no clear dependence of the current layer thickness upon the magnetosheath magnetic field orientation [Berchem and Russell, 1982], we expect growth rates to increase as the shear between the magnetosheath and magnetospheric magnetic fields increases.

Magnetic shear is thought to control the geometry of merging. If one requires the components of the magnetospheric and

<sup>1</sup>Physics Department, Loyola Marymount University, Los Angeles, California

<sup>2</sup>Applied Physics Laboratory, Johns Hopkins University, Laurel, Maryland

<sup>3</sup>Institute for Geophysics and Planetary Physics, University of California at Los Angeles.

magnetosheath magnetic field parallel to the merging line to be equal, then merging occurs along a line passing through the subsolar point whose tilt is uniquely specified [Sonnerup, 1974; Gonzalez and Mozer, 1974]. As shown in Figure 1a, this component merging model predicts that the merging line tilts from southern dawn to northern dusk during periods of southward

and duskward magnetosheath/interplanetary magnetic field orientation. During periods of dawnward IMF, the merging line tilts from northern dawn to southern dusk. As the IMF rotates northward, merging either ceases or continues along a line passing through the subsolar point whose orientation lies close to the (northward) direction of magnetospheric magnetic field. Note that if the requirement concerning the components of the magnetic fields parallel to the merging line is dropped, merging can occur for the full range of shear angles and the subsolar merging line can assume a wide range of orientations [Cowley, 1976].

An alternate assumption to the component model is the assumption that merging occurs at locations where the magnetopause current density maximizes, that is, locations where the magnetosheath and magnetospheric magnetic fields are nearly antiparallel. Figure 1b shows the expected locations of "antiparallel" merging lines for IMF orientations ranging from due southward to duskward and northward [Crooker, 1979; Luhmann et al., 1984]. When the IMF points due southward, merging occurs along an equatorial line. When the IMF gains a duskward component, merging shifts to curves with orientations running from northern dawn to southern dusk in the northern dusk and southern dawn quadrants. As the IMF turns northward, the curves move poleward. Symmetry requires the merging lines during intervals of dawnward IMF to gain southern dawn to northern dusk orientations and lie in the northern dawn and southern dusk quadrants.

Merging may proceed steadily, in bursts, via bursts superimposed upon a steady background rate or via transient diminutions superimposed upon a steady background rate. Bursty merging produces a bubble/flux rope of interconnected magnetosheath and magnetospheric magnetic field lines [Russell and Elphic, 1978]. The newly merged magnetic field lines leave the merging site at high velocities but immediately encounter slowly moving plasma on unmerged magnetic field lines in their surroundings. In response to pressure gradient forces, the velocity of the newly merged magnetic field lines decreases, the surrounding plasma accelerates, and kinetic energy is converted to thermal energy within the bubble/flux rope. The decelerated and heated plasma within the bubbles/flux ropes causes them to swell and disturb the surrounding magnetosheath and magnetospheric regions as they move along the magnetopause [Southwood et al., 1988].

Newly merged magnetic field lines move in response to pressure gradient and magnetic curvature forces [e.g., Crooker, 1979; Cowley and Owen, 1989]. In general, the pressure gradient force points antisunward away from the subsolar point. By contrast, magnetic curvature forces depend upon location and the IMF orientation. When the IMF points duskward, newly merged magnetic field lines connected to the northern ionosphere experience dawnward and northward curvature forces, whereas field lines connected to the southern ionosphere experience duskward and southward curvature forces. When the IMF points dawnward, the sense of the magnetic curvature force reverses.

Summing-up the pressure gradient and curvature forces for the component merging model (Figure 1a), we conclude that during periods of duskward IMF, events observed near the prenoon equator move northward and dawnward, whereas events observed near the postnoon equator move southward and duskward. By symmetry during periods of dawnward IMF orientation, we expect events observed near the prenoon equator to move southward and dawnward, whereas those observed

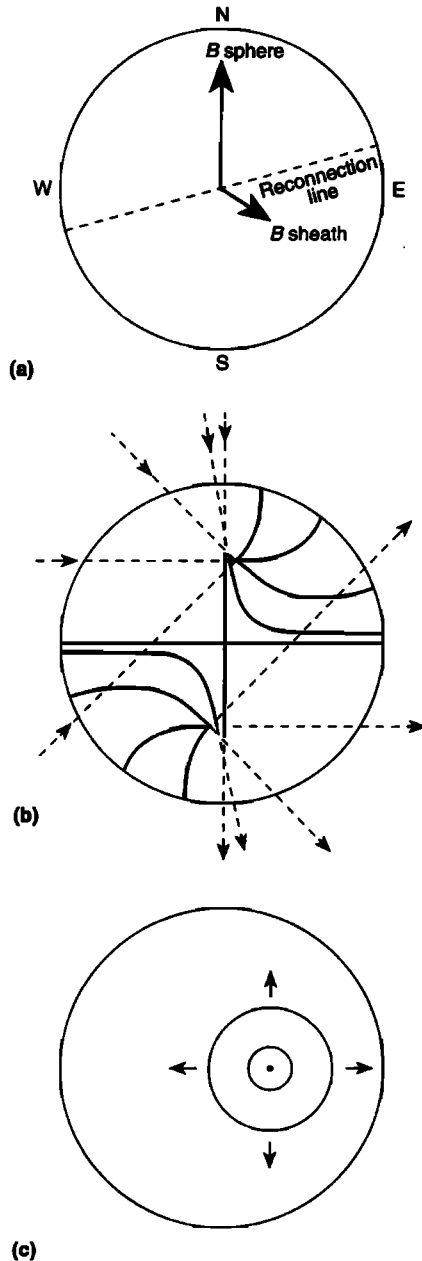


**Figure 1.** (a) Predictions of the component merging model for magnetosheath and magnetospheric magnetic fields of unequal strengths. Merging occurs along a tilted line passing through the subsolar point [Gonzalez and Mozer, 1974]. (b) Predictions of the antiparallel merging model for IMF orientations ranging from due southward to northward and duskward (dashed lines). Merging occurs along the solid curves, which move poleward as the IMF orientation rotates from southward to northward [Crooker, 1979]. (c) Predictions of the pressure pulse model: transient events move radially outward from an initial point of contact on the magnetopause which is not necessarily the subsolar point [Sibeck, 1990].

near the postnoon equator to move northward and duskward. Finally, we note that when curvature forces exceed pressure gradient forces, they may produce sunward moving events (i.e., a duskward moving event observed prior to local noon or a dawnward moving event observed after local noon). This is most likely near local noon, where pressure gradient forces are small and magnetic stresses can be large. However, the component model never produces sunward motion at the equator.

On the basis of merging locations shown in Figure 1b, the antiparallel merging model predicts east-west elongated events moving poleward from the equatorial region during periods of due southward IMF. When the IMF gains a duskward component, the model predicts the formation of events with orientations running from northern dawn to southern dusk in the southern dawn and northern dusk quadrants. To be observed in the equatorial region, such events would have to move northward prior to local noon but southward after local noon. By symmetry, equatorial satellites will observe southward moving events prior to local noon and northward moving events after local noon during periods of dawnward IMF orientation.

### Predictions of the Pressure Pulse Model

*Sibeck* [1990] outlined the predictions of the pressure pulse model. As shown in Figure 1c, the model predicts that variations in the solar wind/foreshock dynamic pressure produce concentric ripples on the magnetopause surface that radiate outward from the point where the pressure pulses first strike the magnetopause. We wish to determine the location of this point for various solar wind discontinuities.

The surfaces of most solar wind discontinuities tend to lie along the IMF spiral [*Siscoe et al.*, 1968], and consequently strike the postnoon bow shock first. Any discontinuity striking the bow shock launches fast mode waves into the magnetosheath that precede the arrival of the discontinuity itself [*Völk and Auer*, 1974; *Hassam*, 1978; *Wu et al.*, 1993]. Fast mode wave speeds in the dayside magnetosheath are comparable to the solar wind velocity, because the bow shock stands along the locus of points where the component of the solar wind velocity along the bow shock normal is identical to the fast mode wave speed in the magnetosheath. Because of these high fast mode wave speeds, the fast mode wave fronts in the magnetosheath keep pace with the discontinuities in the solar wind. During periods of spiral IMF orientation, the fast mode wavefronts should strike first on the postnoon side of the magnetopause. Consequently, the ripples in the magnetopause surface generally emanate from a point displaced duskward from the subsolar point [*Sibeck*, 1990]. During periods of orthospiral IMF, the pressure variations would be expected to strike the prenoon magnetopause first and generate ripples emanating from a prenoon location [e.g., *Korotova and Sibeck*, 1995].

Figure 1c indicates that the orientation of the ripples in the magnetopause surface generally runs from northern dawn to southern dusk in the northern dusk and southern dawn quadrants, but from southern dawn to northern dusk in the northern dawn and southern dusk quadrants. The ripples move poleward when the pressure pulses strike the equatorial magnetopause. Finally, since there is no reason to expect solar wind/foreshock pressure pulses to be more common during periods of northward or southward, dawnward or duskward, IMF orientations, the transient magnetospheric events which they produce must be equally common for all IMF conditions.

### Magnetospheric Signatures of Transient Events on the Magnetopause

Transient events on the magnetopause disturb the magnetospheric magnetic field direction and orientation. Bubbles, flux ropes, and transient increases in the solar wind/foreshock pressure briefly compress the magnetospheric magnetic field, whereas brief decreases in the solar wind/foreshock pressure allow the magnetopause to move outward and the magnetospheric magnetic field strength to decrease. Since transient magnetospheric events are identified on the basis of magnetic field strength increases, we will henceforth consider only the effects associated with bubbles, flux ropes, and pressure pulse increases.

*Farrugia et al.* [1987] modeled the magnetospheric magnetic field perturbations associated with the motion of a two-dimensional cylinder along the magnetopause surface under an assumption of incompressible flow. Northward moving events produce outward/inward bipolar signatures in the component of the magnetic field normal to the nominal magnetopause, whereas southward moving events produce inward/outward signatures. Furthermore, the inward displacement of magnetospheric magnetic field lines during the passage of transient events enhances the component of the magnetospheric magnetic field in the plane of the magnetopause, which lies perpendicular to the event axis. This causes the magnetospheric magnetic field strength to increase and rotate toward the direction perpendicular to the event axis. Magnetic field perturbations within the core region of the event itself depend entirely upon the nature of the current system within the flux rope/bubble.

Of course, it is not entirely clear that FTEs can be modeled as two-dimensional structures. In the original model of *Russell and Elphic* [1978], the events were depicted as true flux ropes penetrating a hole in the magnetopause. If so, the twisted flux tube should be more or less aligned with the ambient field, for example, along the GSM Z axis for encounters with magnetospheric FTEs [*Baumjohann and Paschmann*, 1987].

In any case, transient event signatures observed by satellites within the magnetosphere can be used to determine the direction of motion and orientation of the transient events themselves. Given the strikingly different patterns of event orientation and motion predicted by the pressure pulse, component, and antiparallel merging models, a statistical study of these parameters should immediately determine the dominant cause of transient events.

Determining the direction of event motion relative to the magnetospheric magnetic field is simple because the sense of the magnetic field perturbation normal to the nominal magnetopause can be read from plots of the magnetic field. Determining the orientation of transient events is somewhat more complicated. Following *Elphic and Southwood* [1987] and *Papamastorakis et al.* [1989], we can use the minimum variance analysis routine presented by *Sonnerup and Cahill* [1967] to locate the direction in which the magnetospheric magnetic field component remains constant during the passage of individual transient events. In the limit treated by *Farrugia et al.* [1987], we can equate this direction with the axis of the transient events.

Note, however, that *Walthour et al.* [1993] have recently analyzed the magnetic field perturbations associated with several remotely observed transient events. They found that the direction of the vector associated with the minimum variance of the magnetic field does not lie precisely along the event axis,

but rather is rotated about the true axis by an angle  $\theta_n$ , which depends primarily on a quantity that the authors call the "stretching factor." If  $\theta_n$  is large, the results of the minimum variance routine alone would become useless for our purposes. According to D. W. Walthour (personal communication, 1994), the effect of the stretching factor on  $\theta_n$  becomes very small when the angle between the ambient field direction and the minimum variance direction is greater than about  $60^\circ$ . As will be seen below, our analysis generally provides minimum variance directions which point nearly east-west, whereas the magnetospheric magnetic field orientation is nearly northward. Consequently, we can generally assume that  $\theta_n$  is small and take the minimum variance direction as closely approximating the true axis of the magnetospheric events.

## Data Sets

The AMPTE CCE satellite was launched into a near-equatorial orbit with an  $8.8 R_E$  apogee and a period of 15.7 hours on August 16, 1984. From launch through the end of November 1984, apogee moved from 14.7 to 9.5 LT, affording the satellite an opportunity to make extensive observations in the outer dayside magnetosphere. We used hour-long plots of CCE satellite magnetometer observations [Potemra *et al.*, 1985] plotted in GSE coordinates at 6.2-s resolution to identify transient events in the outer dayside magnetosphere. Once candidate events were identified, we plotted the observations on a larger scale in boundary normal coordinates determined from a minimum variance routine [Sonnerup and Cahill, 1967] run upon the events themselves. We eliminated events which were not marked by bipolar magnetic field signatures normal to the nominal magnetopause centered upon transient magnetic field strength increases.

For comparison with these observations, we used IMP 8 [King, 1982], ISEE 2 [Russell and Elphic, 1978], and AMPTE IRM [Lühr *et al.*, 1985] IMF observations. The IMP 8 observations are 15.36-s averages, the ISEE 2 observations 12-s running averages of 4-s data, and the IRM observations are 5-s averages.

## Case Study

To illustrate the methods employed in this paper, we begin with a case study. From 1000 to 1100 UT on October 28, 1984 (day 302), the CCE satellite moved through the dayside magnetosphere from GSM  $(x,y,z) = (8.5, -0.9, 1.8)$  to  $(8.4, -0.2, 1.6) R_E$ . The lower four panels in Figure 2 shows CCE magnetic field observations in GSM coordinates. There are a series of transient increases in the total magnetic field strength  $B$  centered on the times 1019, 1024, 1034, 1041, and 1051 UT. The  $B_x$  component of the magnetic field rotated from more positive (sunward) to more negative (earthward) values during each of these events. The  $B_y$  component of the magnetic field also became more negative (dawnward) at the time of each event.

ISEE 2 IMF observations are available for the interval under study on this day. The ISEE 2 spacecraft moved radially outward from an initial position at 1000 UT, which was just upstream of the subsolar bow shock at GSM  $(x,y,z) = (18.3, -4.0, -2.8) R_E$ . The top panel of Figure 2 presents ISEE 2 IMF observations in spherical GSM coordinates, where  $\theta = 0$ ,  $\phi = 0$  indicates a sunward pointing magnetic field,  $\theta = 90^\circ$  indicates a northward field, and  $\theta = 0$ ,  $\phi = 90^\circ$  indicates a duskward field. The ISEE 2 observations have been lagged by 6 min, as

determined by comparison with CCE and IRM observations during this interval [Sibeck, 1992]. Like Sibeck [1992] and Sibeck and Newell [1995], we conclude that the CCE events at 1019 and 1024 UT occurred for a southward IMF orientation, the events at 1034 and 1041 UT for a northward IMF orientation, and the event at 1051 UT for a near-ecliptic IMF orientation. We enter these values into Table 1. We present these observations as our example because determining the IMF orientation for the events on this day was more difficult than on other days and depended sensitively on the lag time used. Furthermore, these events correspond in a one-to-one manner to a series of FTEs previously identified in IRM and UKS observations [e.g., Sibeck, 1992].

We ran the Sonnerup/Cahill minimum variance routine over several minute-long intervals of CCE magnetometer observations encompassing the magnetic field strength increases and bipolar signatures within individual transient events. The results for the events shown in Figure 2 have been entered into Table 1. The minimum variance directions for all the events from 1000 to 1100 UT on October 28, 1984, point in  $+y$ ,  $+z$  direction, indicating axes running from southern dawn to northern dusk, as qualitatively determined by Sibeck [1992]. Combining the information that the events moved northward ( $+$ ,  $-B_x$  signature), tilted from southern dawn to northern dusk, and were observed at northern latitudes prior to local noon, we conclude that they moved antisunward, away from the subsolar point and/or locations further duskward and southward. This conclusion is consistent with the fact that they were observed by the IRM satellite some 4 min later at a location northward and dawnward of the CCE [Sibeck, 1992].

We now compare the characteristics of the events to those predicted by the pressure pulse, component, and antiparallel merging models. Figure 2 shows that the IMF longitude at the times of the events ranged from nearly sunward and slightly dawnward ( $\phi \sim -10^\circ$ ) to sunward and dawnward ( $\phi \sim -60^\circ$ ). Solar wind features with this orientation would be expected to strike the postnoon magnetopause first and then reach the subsolar point. The pressure pulse model predicts that transient events will move northward and dawnward (i.e., antisunward) past satellites located prior to local noon and north of the geomagnetic equator. Furthermore, the model predicts event axes running from southern dawn to northern dusk in the northern prenoon quadrant. These predictions are in accord with the CCE and IRM observations [Sibeck, 1992].

Some of the observations are inconsistent with the component merging model. During the period under study, the IMF pointed either slightly or strongly dawnward. The component merging model predicts event generation along a tilted subsolar line running from northern dawn to southern dusk during periods of dawnward IMF. Observed event axes run from southern dawn to northern dusk. Furthermore, the model predicts that the inclination of the event axis from the equatorial plane will increase as the IMF rotates northward. The first two events on this day occurred during an interval of southward IMF orientation, whereas the second two occurred during an interval of northward IMF orientation. The tilts derived from the minimum variance routine do not differ in the expected manner. Finally, the model predicts that events will not occur during periods of strongly northward IMF orientation. However, events continued to occur during the periods of northward IMF orientation shown in Figure 2.

The characteristics of the events are also inconsistent with some of the predictions of the antiparallel merging model. That model predicts event formation near the equatorial plane during

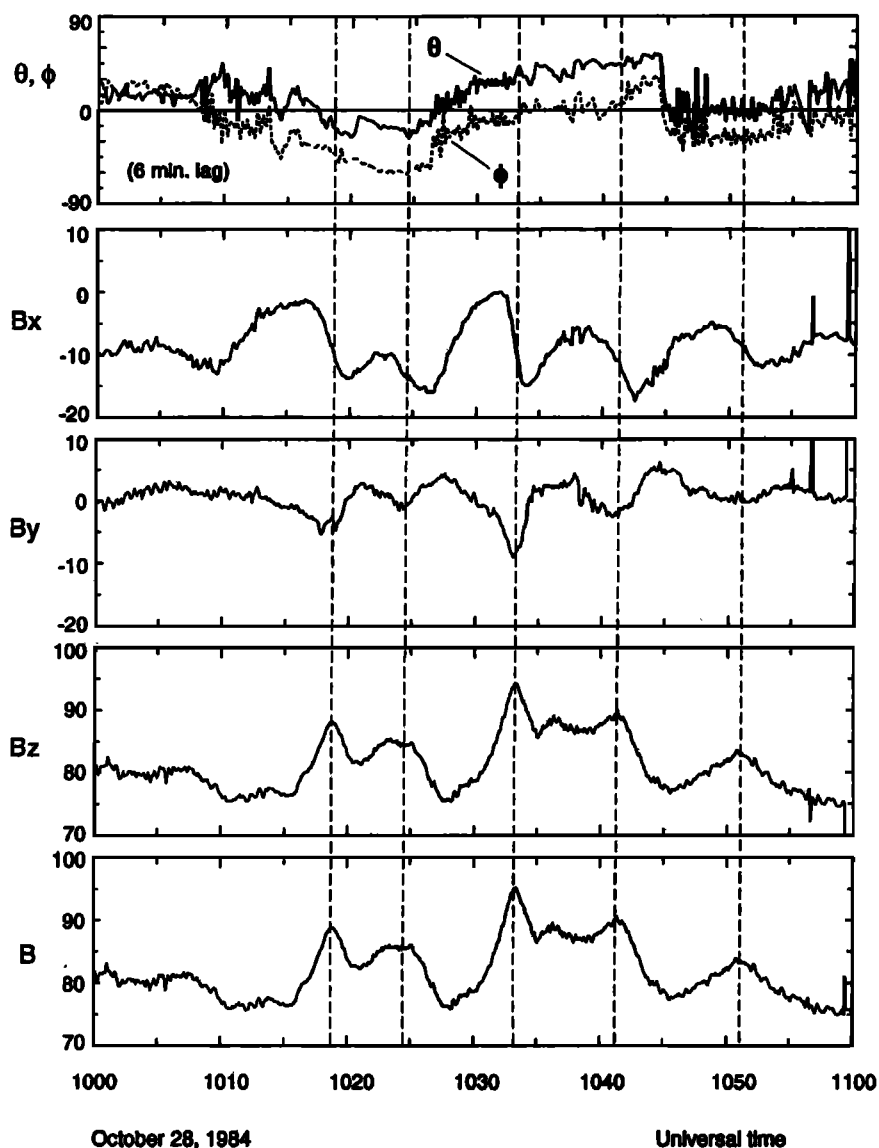


**Figure 2.** A comparison of ISEE 2 IMF and CCE magnetospheric magnetic field observations in GSM coordinates during the interval from 1000 to 1100 UT on October 28, 1984. The ISEE 2 observations have been lagged 6 min on the basis of a previous comparison with IRM observations [Sibeck, 1992].

periods of strongly southward IMF and at higher latitudes during periods of ecliptic and strongly northward IMF. The IMF never pointed strongly southward during the interval under study, yet the sense of the bipolar signature observed normal to the magnetopause led us to conclude that all the events were moving northward away from the geomagnetic equator. However, the model also predicts event orientations running from southern dawn to northern dusk during periods of dawnward IMF orientation, as observed on this day.

Finally, note that the observations shown in Figure 2 indicate that the CCE observes events on October 28, 1984, with similar recurrence and duration times. Each of these CCE events corresponds to a much more clearly defined transient event in UKS/IRM observations further radially outward [e.g., Lockwood *et al.*, 1988]. However, the UKS/IRM observations for this day indicate events with significantly longer recurrence than duration times. Russell and Elphic [1978] have also reported much more sharply defined classic FTE signatures observed in the vicinity of the magnetopause. Perhaps, as dis-

cussed below, the short wavelengths that define individual transient events at the magnetopause decay more rapidly with distance inward from the magnetopause than do the long-wavelength components, which define their recurrence times.

Since many arguments might be advanced as to whether or not the events and observations on this day were typical, it is essential to continue with a statistical study.

### Statistical Survey

**Event selection criteria.** We examined CCE magnetometer observations at radial distances from Earth exceeding  $8.0 R_E$  on all satellite orbits from August through November 1984. We identified 59 events marked by peak-to-peak bipolar fluctuations in the GSE  $B_x$  component exceeding 4 nT, rotations of the magnetic field component in the  $Y$ - $Z$  plane, increases in the magnetic field strength, and durations greater than 1 min. Using the GSE  $B_x$  component to identify bipolar magnetic field signatures normal to the nominal magnetopause is justified on

Table 1. List of Events

Day	Time, UT	Position,* $R_g$	Min. Var. Axis <sup>b</sup>	Motion <sup>c</sup>	IMF $B_x$	IMF $B_y$	IMF $B_z$	IMF Source
230	1223	(2.66, -2.01)	[0.900, 0.316]	S, ASw	>0	<0	>0	IMP
232	1155	(2.84, -2.06)	[0.916, -0.233]	S, ASw	>0	>0	<0	IRM
	1234	(3.45, -2.20)	[0.881, 0.029]	S, ASw	>0	>0	<0	IRM
234	1123	(3.46, -2.19)	[0.855, 0.462]	S, ASw	>0	>0	<0	IRM
236	1337	(5.48, -2.23)	[0.229, 0.966]	S, ASw	<0	>0	<0	IRM
	1418	(5.75, -2.04)	[0.386, 0.873]	S, ASw	<0	>0	<0	IRM
	1504	(5.95, -1.76)	[0.511, 0.830]	S, ASw	<0	>0	>0	IRM
	1512	(5.97, -1.70)	[0.510, 0.736]	S, ASw	<0	>0	>0	IRM
	1543	(6.00, -1.46)	[0.909, 0.330]	S, ASw	<0	>0	<0	IRM
241	1457	(2.55, -1.44)	[0.969, -0.229]	S, ASw	<0	>0	disturbed	ISEE
	1613	(3.69, -1.39)	[0.984, 0.170]	S, ASw	<0	>0	<0	IMP
243	0321	(5.65, -0.77)	[0.731, 0.239]	N, ASw	<0	>0	<0	IMP
244	2144	(2.95, -0.56)	[0.951, 0.097]	S, ASw	<0	>0	>0	ISEE
249	0922	(0.38, -0.77)	[0.982, -0.104]	S, ASw	>0	>0	<0	IRM
	1610	(5.13, -1.11)	[0.615, 0.768]	N, Sw	>0	<0	<0	IRM
	1632	(5.23, -0.98)	[0.811, 0.543]	N, Sw	>0	<0	<0	IRM
251	0955	(1.64, -1.13)	[0.989, -0.106]	S, ASw	>0	<0	>0	IRM
254	1547	(1.17, -0.67)	[0.924, -0.310]	S, ASw	>0	<0	<0	ISEE
	1555	(1.25, -0.67)	[0.990, -0.139]	S, ASw	>0	<0	<0	ISEE
	1643	(1.91, -0.69)	[0.999, 0.028]	S, ASw	>0	<0	<0	ISEE
	1649	(2.05, -0.69)	[0.953, -0.295]	S, ASw	>0	disturbed	<0	ISEE
255	0736	(1.13, -0.75)	[0.909, -0.414]	S, Sw	>0	<0	>0	ISEE
256	1418	(0.56, -0.55)	[0.988, -0.098]	S, ASw	>0	>0	<0	IRM
	1427	(0.63, -0.56)	[0.978, -0.148]	S, ASw	>0	<0	>0	IRM
	1438	(0.86, -0.60)	[0.995, -0.062]	S, ASw	>0	<0	<0	IRM
	1449	(1.00, -0.62)	[0.995, -0.075]	S, ASw	>0	<0	>0	IRM
258	1701	(3.31, -0.57)	[0.993, -0.096]	S, ASw	disturbed	disturbed	disturbed	IRM
	1713	(3.47, -0.55)	[0.640, 0.769]	S, ASw	disturbed	disturbed	disturbed	IRM
263	2107	(2.00, 0.03)	[0.968, -0.179]	N, ASw	<0	>0	>0	ISEE
	2138	(2.42, 0.10)	[0.985, -0.158]	N, Sw	<0	>0	<0	ISEE
	2158	(2.65, 0.13)	[0.967, 0.084]	S, ASw	<0	>0	>0	ISEE
	2214	(2.81, 0.16)	[0.952, 0.185]	N, Sw	<0	>0	>0	ISEE
264	1233	(1.66, -0.55)	[0.999, 0.013]	N, Sw	<0	>0	<0	ISEE
	1242	(1.84, -0.59)	[0.969, 0.115]	N, Sw	<0	>0	<0	ISEE
265	2016	(1.93, 0.07)	[0.918, 0.014]	S, ASw	<0	>0	>0	IRM
278	2132	(0.43, 0.69)	[0.995, 0.097]	S, ASw	>0	disturbed	<0	IMP
	2303	(1.62, 0.70)	[0.776, -0.561]	N, ASw	>0	<0	<0	IMP
281	1439	(2.17, 0.23)	[0.902, 0.279]	S, ASw	>0	<0	>0	IRM
283	0916	(-0.97, 0.97)	[0.872, 0.483]	S, Sw	>0	>0	disturbed	IRM
	0933	(-0.75, 0.92)	[0.974, 0.124]	N, ASw	>0	<0	>0	IRM
290	1337	(-1.63, 1.32)	[0.879, -0.401]	N, Sw	<0	>0	<0	IRM
	1711	(0.71, 0.99)	[0.965, -0.261]	N, Sw	<0	>0	<0	ISEE
	1753	(1.21, 0.97)	[0.969, 0.103]	N, Sw	<0	>0	<0	ISEE
294	1340	(-0.55, 1.34)	[0.986, 0.140]	N, ASw	<0	>0	<0	IRM
302	1018	(-0.64, 1.76)	[0.776, 0.511]	N, ASw	>0	<0	<0	ISEE
	1024	(-0.63, 1.72)	[0.908, 0.417]	N, ASw	>0	<0	<0	ISEE
	1033	(-0.51, 1.69)	[0.607, 0.630]	N, ASw	>0	<0	>0	ISEE
	1041	(-0.42, 1.65)	[0.840, 0.542]	N, ASw	>0	<0	>0	ISEE
	1051	(-0.33, 1.63)	[0.884, 0.466]	N, ASw	>0	<0	<0	ISEE
	1121	(0.03, 1.51)	[0.973, 0.082]	N, Sw	>0	<0	>0	ISEE
	1205	(0.56, 1.31)	[0.967, -0.260]	N, Sw	>0	disturbed	>0	ISEE
	1213	(0.67, 1.28)	[0.977, 0.057]	N, Sw	>0	<0	>0	ISEE
307	0220	(0.18, 1.50)	[0.988, 0.119]	N, SW	>0	<0	>0	IMP
	0239	(0.47, 1.46)	[0.991, 0.121]	N, Sw	>0	<0	>0	IMP
	0254	(0.70, 1.42)	[0.985, -0.144]	N, Sw	>0	>0	>0	ISEE
	1036	(-3.92, 2.14)	[0.816, 0.402]	N, ASw	>0	<0	>0	ISEE
308	0847	(-0.19, 1.73)	[0.806, -0.591]	N, Sw	>0	>0	>0	IRM
316	0525	(-0.59, 1.85)	[0.994, 0.106]	S, Sw	>0	>0	>0	IRM
	0555	(-0.10, 1.73)	[0.966, 0.108]	N, ASw	>0	<0	>0	IRM

\*Coordinates in the yz GSM plane.

<sup>b</sup>The y and z components of the minimum variance axis unit vector.<sup>c</sup>N, S, north, south; ASW, Sw, antisunward, sunward.

the grounds that normals to the Earth's magnetopause in the vicinity of local noon point nearly along the Earth-Sun line, and "the identification of FTEs is not sensitively dependent on the direction of the normal" [Rijnbeek *et al.*, 1984].

Figure 3 shows a histogram of peak-to-peak amplitudes for the CCE events. Peak-to-peak amplitudes ranged from 4 to 27

nT, with a median amplitude of 10 nT. Figure 4 shows a histogram of event duration  $\tau$ . Like Kawano *et al.* [1992], we define the duration as the time between peak positive and negative deflections in the component of the magnetic field normal to the nominal magnetopause. Kawano *et al.* [1992] distinguished between events with durations longer and shorter than

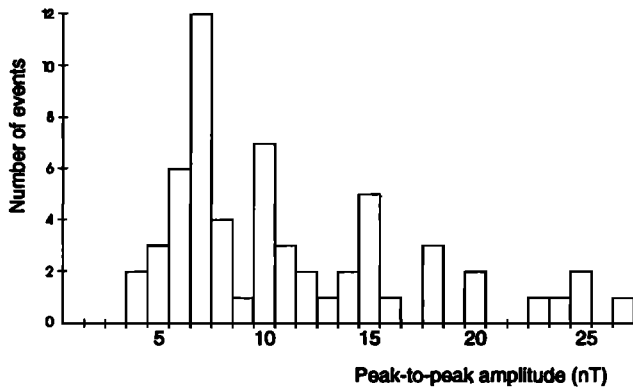


**Figure 3.** A histogram of the peak-to-peak bipolar  $B_x$  amplitudes for the 59 transient magnetospheric events in this study.

1.5 min. Of the 59 events we studied, 6 have durations less than 1.5 min and 53 have durations in excess of 1.5 min. In one case, the duration was as large as 8 min.

Because we wish to compare the results of our survey with those previously reported, it is worthwhile noting the criteria that previous authors have used to identify transient events. *Kawano et al.* [1992] used CCE observations to identify magnetospheric events at radial distances beyond  $6.0 R_E$ , which were marked by bipolar signatures in the radial component of the magnetic field centered on increases in the total magnetic field strength. Peak-to-peak variations in the radial component and magnetic field strength were required to exceed 3 nT, and the duration of the events was required to exceed 1 min. Some events lasted as long as 15 min. Our criteria are essentially identical to those of *Kawano et al.* [1992], except that we only consider events at the greatest radial distances reached by the CCE and exclude events with durations greater than 8 min.

*Berchem and Russell* [1984] identified events in ISEE 1/2 observations of the magnetosheath on the basis of sudden strong enhancements in the total magnetic field, bipolar inward/outward or outward/inward signatures in the component of the magnetic field normal to the nominal magnetopause, and rotations of the component of the field tangential to the magnetopause towards directions neither along the magnetosheath nor the magnetospheric magnetic field. *Kuo et al.* [1995] identified isolated events with greater than 10 nT peak to peak bipolar signatures in the normal component and durations greater than 30s.

*Rijnbeek et al.* [1984] and *Southwood et al.* [1986] surveyed ISEE 1/2 and UKS observations, respectively. By contrast to *Berchem and Russell* [1984], they included magnetosheath and magnetospheric events which were marked by asymmetric bipolar, monopolar, and more complex signatures in the component of the magnetic field normal to the magnetopause, those in which the tangential field does not rotate toward the direction on the other side of the magnetopause, and those in which the components of the magnetic field in the plane of the magnetopause exhibit large-scale oscillatory changes. Like *Kuo et al.* [1995], they also included a small number of events in which there was no obvious increase in the magnetic field strength. The peak-to-peak variation in the magnetic field component normal to the nominal magnetopause was required to exceed 10 nT and 20 nT during intervals of high field strength, and the minimum event duration was 1 min.

Our criteria are more stringent than those used by *Rijnbeek et al.* [1984], *Southwood et al.* [1986], and *Kuo et al.* [1995],

because we include only transient events with "classical" signatures, including magnetic field strength increases. Furthermore the weak  $>4$  nT amplitudes, which we use to identify events at the CCE orbit, correspond to events with much stronger signatures in the vicinity of the magnetopause. Event amplitudes decay with distance from a planar magnetopause at a rate proportional to  $e^{-2\pi x/\lambda}$ , where  $x$  is the distance from the magnetopause and  $\lambda$  the characteristic wavelength. For a subsolar magnetopause located at  $10.8 R_E$  [e.g., *Fairfield*, 1971], the CCE apogee of  $8.8 R_E$ , and events with dimensions of  $\sim 4 R_E$  along the magnetopause ( $\lambda = 8 R_E$ ), our minimum amplitude of 4 nT at CCE orbit corresponds to events with amplitudes of at least 20 nT at the magnetopause.

**Location and north/south direction of motion.** The base of each arrow in Figure 5 presents the location where each of the 59 events occurred in GSM coordinates. The CCE orbit confines observations south of the equator to local times after local noon, but observations north of the geomagnetic equator to local times at and before local noon (see also Figure 6 of *Kawano et al.*, [1992]).

The arrows are coded according to the sense of the bipolar  $B_x$  signature observed at the time of each event. Solid arrows indicate standard (or northward moving) events which were accompanied by bipolar outward/inward signatures in the  $B_x$  component, whereas dashed arrows indicate reverse (or southward moving events) which were accompanied by bipolar inward/outward signatures. There is a marked tendency for northward moving events to occur north of the geomagnetic equator and southward moving events to occur south of the geomagnetic equator. Of 29 events which occurred north of the geomagnetic equator, 23 are standard and 6 reverse. In contrast, of 30 events which occurred south of the geomagnetic equator, 25 are reverse and 5 standard. Furthermore, those standard events south of the equator and reverse events north of the equator tended to occur in the immediate vicinity of the equator. These results lead to the conclusion that most events move away from the geomagnetic equator.

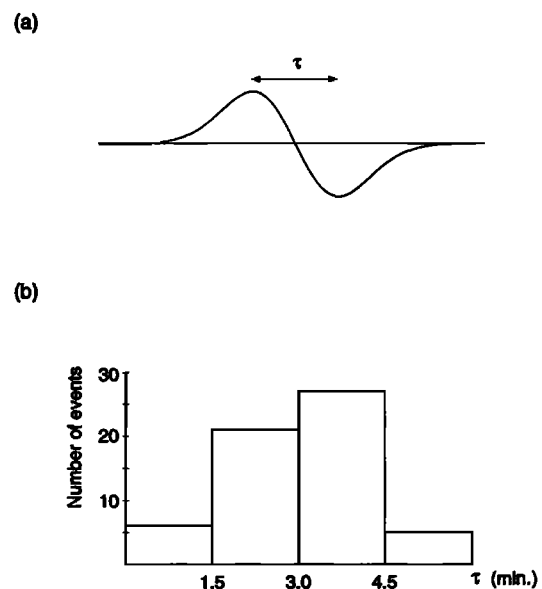


**Figure 4.** (a) The definition of event duration ( $\tau$ ) used in this study. (b) A histogram of the durations for the 59 events in this study.



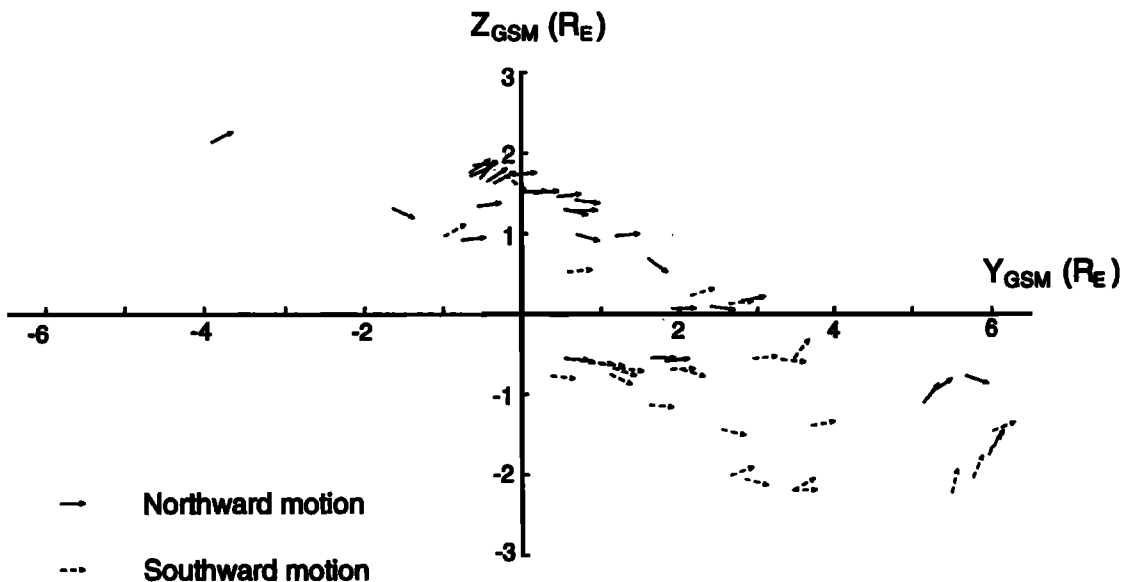


**Figure 5.** The locations and orientations of the 59 events in this study plotted in the GSM  $y$ - $z$  plane. Solid vectors are standard events marked by bipolar outward/inward signatures normal to the magnetopause, whereas dashed vectors are reverse events marked by bipolar inward/outward signatures. The events were observed in the equatorial regions, most move poleward, and most have axes which lie nearer the  $y$  axis than the  $z$  axis.

**Event orientation.** We used the minimum variance routine discussed by *Sonnerup and Cahill* [1967] to determine the orientation of each of the 59 transient magnetospheric events in this study. Figure 5 presents the results of this survey as a function of position in the GSM  $Y$ - $Z$  plane. As the figure indicates, most of the events have orientations lying more nearly parallel to the  $Y$  axis than the  $Z$  axis. The exceptions to this generalization are the transient events studied above, which occurred on October 28, 1984, near GSM  $(Y, Z) = (-0.5, 1.8) R_E$ , and several transient events which occurred near GSM  $(Y, Z) = (5.5, -1.5) R_E$ .

Figure 6 presents a histogram of the event orientation as a function of latitude away from the  $+Y$  GSM axis in the  $Y, Z$

GSM plane. Nearly half (27 of 59, or 46%) of the events had axes which lay within  $\pm 10^\circ$  of the  $y$  axis, and over two-thirds (40 of 59, or 68%) of the event axes lay within  $\pm 20^\circ$  of the equator. Thus most event axes tend to lie in an east-west direction rather than north-south. Note that the absence of events with north-south orientations may be an artifact of our event selection criteria. The motion of events whose axes lie nearly along the magnetospheric magnetic field (if there are such events) would not produce significant bipolar signatures normal to the nominal magnetopause.

**Event occurrence and orientation as a function of IMF direction.** We now wish to consider the characteristics of the transient magnetospheric events as a function of the IMF orien-

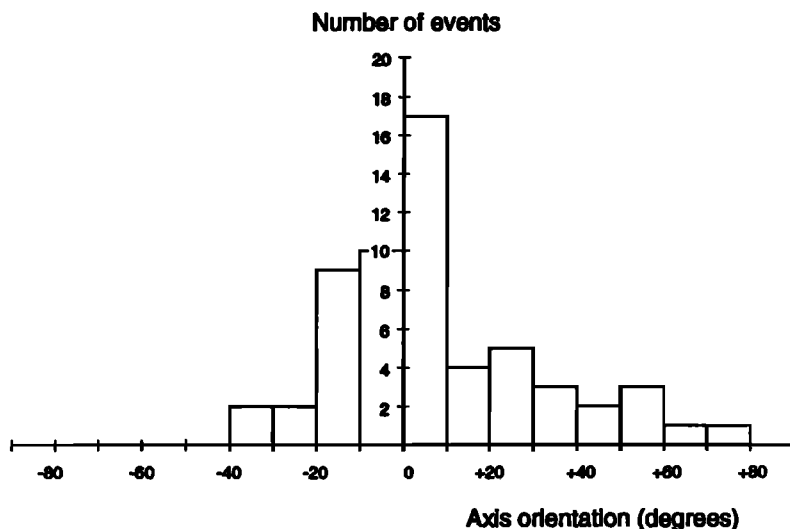


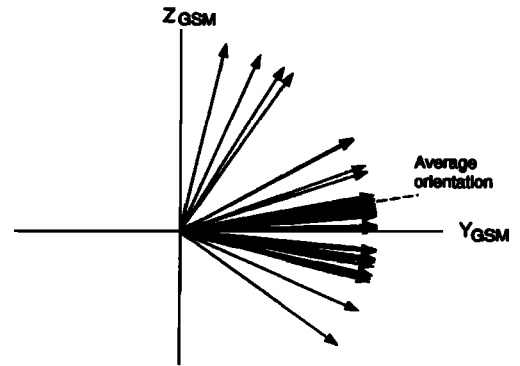
**Figure 6.** A histogram of event orientation as a function of latitude away from the  $Y$  axis in the  $Y$ - $Z$  GSM plane.

tation. *Sibeck and Newell* [1995] reviewed the various methods used in the past to infer the interplanetary/magnetosheath magnetic field orientation at the times of transient magnetospheric events, showed that they yield remarkably different results, and identified several reasons for the discrepancies. Previous authors averaged 30-min stretches of magnetosheath and solar wind magnetic fields to determine the predominant orientation [Rijnbeek *et al.*, 1984; Southwood *et al.*, 1986; Kawano *et al.*, 1992]. The magnetic field orientation may not have remained constant throughout these intervals, and the average orientation may not be that at the time of the transient event. The magnetosheath magnetic field may differ greatly from that predicted on the basis of upstream observations during rare intervals of nearly radial IMF orientation, and IMF features often exhibit short scale lengths transverse to the Earth-Sun line.

We inspected plots of IMP 8, ISEE 2, and IRM magnetometer observations during the 10-min interval preceding each transient magnetospheric event. Because IMP 8 often lay far off the Earth-Sun line at the times of the events studied, whereas ISEE 2 and IRM were generally upstream of the sub-solar bow shock [e.g., Bryant *et al.*, 1985; Sibeck and Newell, 1995], we chose to use IMF observations by the latter satellites whenever possible. Previous experience indicates that IMF scale lengths can be less than the distance separating IMP 8 from the Earth-Sun line [e.g., Lanzerotti, 1989; Sibeck *et al.*, 1989b; Sibeck, 1992].

Entries in Table 1 note the sense of each IMF component and whether or not they varied during the 10-min interval preceding each event. Events which occurred during intervals of highly variable IMF orientation, or when an IMF component was near zero, were omitted from the surveys as a function of IMF  $B_y$  and  $B_z$ , respectively. Figure 7a presents a plot of transient magnetospheric event occurrence as a function of IMF  $B_y$ ; Figure 7b presents the occurrence pattern as a function of IMF

(a)  $B_y > 0$



(b)  $B_y < 0$

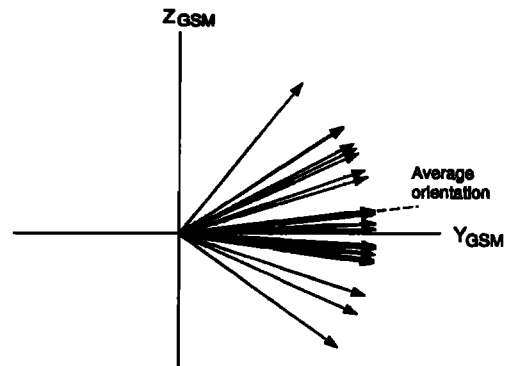


**Figure 8.** Event axis orientation as a function of IMF  $B_y$ . The top panel shows the event orientations for IMF  $B_y > 0$ . The lower panel shows observed orientations for IMF  $B_y < 0$ .

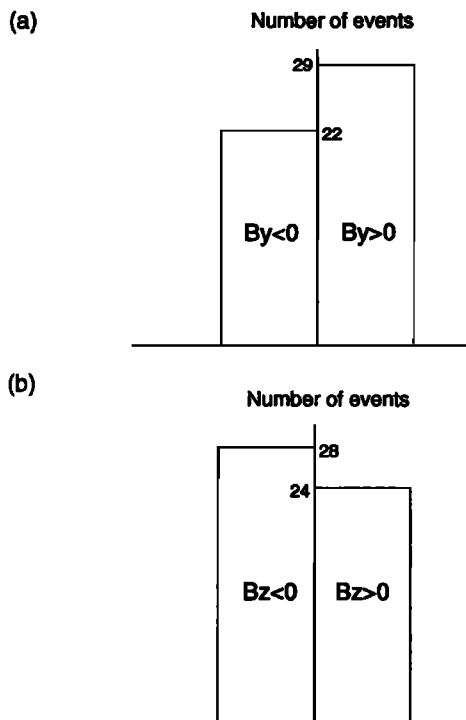


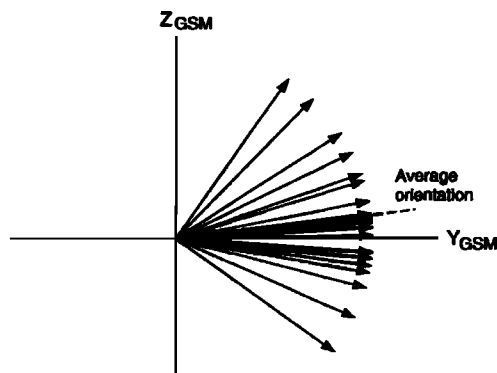
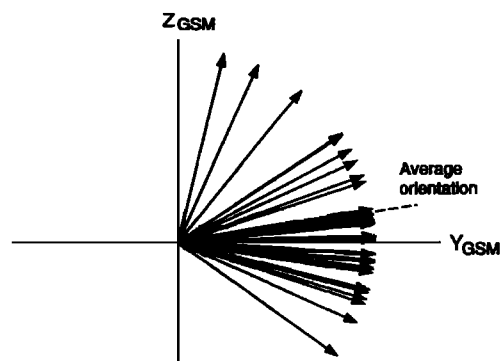
**Figure 7.** (a) Event occurrence as a function of IMF  $B_y$ . (b) Event occurrence as a function of IMF  $B_z$ .

$B_z$ . Slightly more than half the events occurred during intervals of positive IMF  $B_y$ , and slightly more than half during intervals of negative  $B_z$ . We conclude that events are equally likely for north and south, downward and duskward, IMF orientations.

Figure 8 presents information concerning event axis orientation as a function of IMF  $B_y$ . The top panel shows the results for 29 events that occurred during intervals of positive IMF  $B_y$ , whereas the bottom panel shows the results for 22 events that occurred during intervals of negative IMF  $B_y$ . There is little difference between the two panels. For both IMF orientations, event axes tend to cluster around the +Y GSM axis. The average inclinations of the event axes from the +Y axis are  $9^\circ$  and  $7^\circ$  for positive and negative IMF  $B_y$ , respectively. These results indicate that IMF  $B_y$  has little, if any, control over the event orientation.

Figure 9 presents information concerning event axis orientation as a function of IMF  $B_z$ . The top panel shows the results for 24 events that occurred for positive IMF  $B_z$ , and the bottom panel shows the results for 28 events that occurred for negative IMF  $B_z$ . The average inclinations of the event axes from the +Y axis are  $6.5^\circ$  and  $8.4^\circ$  for positive and negative IMF  $B_z$ , respectively. The results indicate that IMF  $B_z$  has little or no control over the orientation of transient event axes.

**IMF orientation and the direction of event motion.** As noted by Kawano *et al.* [1992], information about event orientation and north/south direction of motion can also be used to infer eastward and westward motion. Events with orientations running from southern dawn to northern dusk which move

(a)  $B_z > 0$ (b)  $B_z < 0$ 

**Figure 9.** Event axis orientation as a function of IMF  $B_z$ . The top panel shows the event orientations for IMF  $B_z > 0$ . The lower panel shows observed orientations for IMF  $B_z < 0$ .

northward also have a westward component of motion. Events with the same orientation which move southward also have an eastward component of motion. By symmetry, events with an orientation running from northern dawn to southern dusk which move northward also move duskward. Events with the same orientation which move southward also move dawnward.

Table 1 identifies all sunward and antisunward moving events in our data set. The vast majority of the events (40 of 59) moved antisunward, that is, dawnward prior to local noon or duskward after local noon. However, 4 of 13 events prior to local noon moved duskward and 15 of 46 events after local noon moved dawnward. We interpret these as sunward moving events.

Merging models explain duskward moving events observed prior to local noon and dawnward moving events after local noon in terms of magnetic curvature forces, whereas the pressure pulse model explains them in terms of pressure pulses striking the magnetopause at locations away from the subsolar point. We wish to test the ability of both models to explain the sunward moving events.

During periods of duskward IMF orientation, magnetic curvature forces pull events connected to the northern hemisphere dawnward. During periods of dawnward IMF orientation, the same forces pull events connected to the northern hemisphere duskward. If we interpret northward moving events as those connected to the northern hemisphere, we find 14 such events moving sunward after local noon and 2 prior to local noon. Of the 14 events, 7 occurred for positive IMF  $B_y$  (consistent with

merging model predictions), 2 for IMF  $B_y$  near zero or disturbed, and 5 for negative IMF  $B_y$ . Neither of the two events observed moving northward and sunward prior to local noon occurred for the negative IMF  $B_y$  predicted by the merging models.

During periods of dawnward IMF orientation, magnetic curvature forces pull events connected to the southern hemisphere dawnward. During periods of duskward IMF orientation, the same forces pull events connected to the southern hemisphere dawnward. If we interpret southward moving events as those connected to the southern hemisphere, we find 2 moving sunward prior to local noon and 1 after local noon. Both of the two events which were noted moving sunward prior to local noon occurred during intervals of positive IMF  $B_y$ , consistent with the predictions of the merging models. The event noted after local noon moving sunward occurred for a negative IMF  $B_y$ , also consistent with the predictions of the merging models.

Summarizing the results, the sense of the IMF  $B_y$  component sufficed to explain the motion of 10 of the 19 sunward moving events, but failed to do so for 7 of the events. The IMF  $B_y$  component was disturbed or near zero for two of the events.

Now we test the predictions of the pressure pulse model, which predicts sunward moving events just after local noon during periods of spiral IMF orientation ( $B_x > 0$  and  $B_y < 0$  or  $B_x < 0$  and  $B_y > 0$ ) and sunward moving events just prior to local noon during periods of orthospiral IMF orientation. Figure 10 presents the locations where sunward moving events were observed during periods of spiral IMF orientation (top panel) and orthospiral IMF orientation (bottom panel). Of the 15 sunward moving events observed after local noon, 12 occurred during intervals of spiral IMF orientation (consistent with pressure pulse model predictions), one for an orthospiral IMF orientation, and 2 for a disturbed or near zero IMF  $B_y$  component (not shown). Of the 4 sunward moving events observed prior to local noon, 3 occurred for an orthospiral IMF orientation (consistent with pressure pulse model predictions) and one for a spiral IMF orientation. The pressure pulse model satisfactorily explains the sunward motion of all but two of the events for which the IMF orientation was well determined.

Summarizing the results of the surveys concerning the direction of event motion, we find that the pressure pulse model explained a greater fraction of the sunward moving events for which the IMF orientation was clearly defined (15/17 or 88%) than did the merging models (10/17 or 59%).

## Discussion and Comparison with Previous Work

The results presented in this paper lead to three key conclusions: (1) the transient magnetospheric events in our data set are east/west aligned and originate near the geomagnetic equator, (2) event occurrence and alignment do not depend upon the IMF orientation, and (3) event motion is better explained in terms of the spiral/orthospiral IMF orientation than magnetic curvature forces associated with IMF  $B_y$ . Here we consider the characteristics of the events within the framework of the component, antiparallel, and pressure pulse models.

Interpreted in terms of component merging, the east/west alignment of the transient events presented in this paper eliminates an explanation in terms of flux ropes with narrow longitudinal dimensions penetrating a hole in the magnetopause [e.g., Baumjohann and Paschmann, 1987]. Instead, it argues in favor of the extended two-dimensional structures proposed by Farrugia

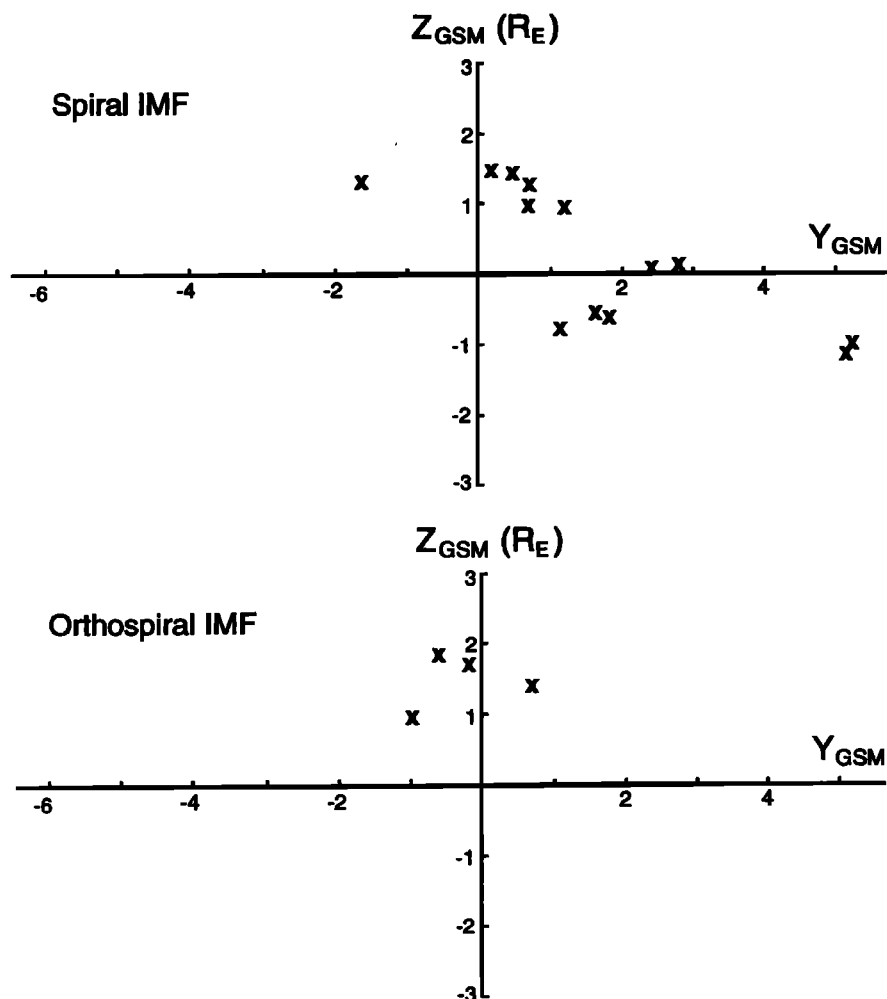


**Figure 10.** Locations where sunward moving events were observed for (a) spiral IMF orientations, (b) orthospiral IMF orientations. The locations agree with the predictions of the pressure pulse model.

*et al.* [1987]. Furthermore, the observations presented in this paper require the structures to form along a component merging line that lies nearly along the equatorial magnetopause for both northward and southward IMF orientations and remains there without any tilting in response to variations in IMF  $B_y$  or  $B_z$ . The observations also require a significant number of transient events to move sunward in response to some force other than magnetic curvature. Since these are not the predictions of the component merging model, we conclude that the characteristics of the transient events studied in this paper are inconsistent with an interpretation in terms of component merging.

Bursty antiparallel merging models predict the production of transient events along off-equatorial merging lines whose orientation depends upon the IMF direction. The results presented in this paper are inconsistent with an interpretation in terms of antiparallel merging, because the events appear to originate along an equatorial line whose orientation does not depend upon the IMF direction. Although the events continue to occur for both northward and southward IMF orientations, a feature consistent with an interpretation in terms of antiparallel merging, the sense of the magnetic curvature forces only accounts for the sunward motion of about half of the events, a fraction which would be expected to occur by chance.

The events studied in this paper are more easily explained in terms of a pressure pulse model. The pressure pulse model

predicts poleward moving events at prenoon and postnoon local times, sunward moving events at early postnoon local times during the relatively common spiral IMF periods, and sunward moving events at late prenoon local times during the relatively rare intervals of orthospiral IMF orientation. The model predicts no dependence of event occurrence or orientation upon the north/south component of the IMF. We noted all of these features in the survey above.

Nevertheless, numerous case and statistical studies have interpreted transient events in terms of bursty merging. We should try to reconcile our observations with this work. For example, *Rijnbeek et al.* [1984], *Berchem and Russell* [1984], and *Kuo et al.* [1995] reported that transient events in the vicinity of the magnetopause show a strong tendency to occur during periods of southward IMF orientation. *Daly et al.* [1984] and *Russell et al.* [1985] interpreted transient event spatial occurrence patterns in terms of a tilted subsolar merging line. Case studies of event orientation provided evidence consistent with the component merging model [*Elphic and Southwood*, 1987; *Papamastorakis et al.*, 1989].

On the other hand, several studies presented results inconsistent with bursty magnetic merging. *Kawano et al.* [1992] reported that events with durations greater than 1.5 min, which were observed by the CCE satellite in the outer dayside magnetosphere, showed little tendency to occur during intervals of

southward IMF orientation, whereas events with durations less than 1.5 min did show such a tendency. *Borodkova et al.* [1995] reported no tendency for transient events observed at geosynchronous orbit to occur during periods of southward IMF orientation.

There is a way to reconcile the apparent discrepant observations. Note that all the events considered by *Daly et al.* [1984], *Rijnbeek et al.* [1984], *Berchem and Russell* [1984], *Elphic and Southwood* [1987], *Papamastorakis et al.* [1989], and *Kuo et al.* [1995] were observed by the ISEE 1/2 or IRM satellites in the immediate vicinity of the magnetopause, whereas the studies which reported no tendency for transient events to occur during periods of southward IMF orientation relied upon CCE and geosynchronous observations deep within the magnetosphere. Since the amplitude of the perturbations associated with transient events decays with distance from the magnetopause, satellites deep within the magnetosphere can observe only those events with the greatest amplitudes. Given the lack of any IMF dependence, these events must be interpreted in terms of pressure pulse driven magnetopause motion.

However, there could be many more transient events with small amplitudes in the immediate vicinity of the magnetopause. Given the reported tendency of transient events at the magnetopause to occur preferentially during periods of southward IMF orientation, these events can still be interpreted in terms of bursty merging.

To pursue this suggestion, we considered the occurrence pattern of those events in our own data set with the shortest duration. Of the 59 events in this study, only 6 have durations less than 1.5 min (Figure 4). Of these 6 events, 4 occurred for a southward IMF orientation, 1 for a fluctuating north/south orientation, and one for a northward IMF orientation. Thus, like *Kawano et al.* [1992], we find that the CCE satellite tends to observe transient events with duration less than 1.5 min when the IMF has a southward component. This indicates either that events with short periods are most commonly generated during intervals of southward IMF orientation, or that events with short durations have weak amplitudes and can only be observed by the CCE satellite when the IMF is southward and the magnetopause has moved radially inward.

## Conclusion

We began this paper by outlining the predictions of the pressure pulse, component, and antiparallel merging models concerning the occurrence patterns, motion, and orientation of transient events in the outer dayside magnetosphere. Both merging models predict enhanced transient event occurrence rates in the equatorial regions during periods of strongly southward IMF orientation and events moving sunward in response to magnetic curvature forces.

The component and antiparallel merging models predict differing patterns of event orientation as a function of the IMF direction. During periods of duskward IMF orientation, the component merging line runs from southern dawn to northern dusk, whereas antiparallel merging lines in the southern dawn and northern dusk quadrants run from northern dawn to southern dusk. Events generated along an extended longitudinal portion of the merging line should acquire the orientation of that line. Localized merging may produce a flux rope passing through a hole in the magnetopause, in which case the corresponding magnetospheric event would have a strong north/south orientation.

To be observed, transient events must move away from the point of origin, whereas the component merging model predicts event motion away from a tilted merging line, the antiparallel merging model predicts merging at off-equatorial locations under most conditions. Consequently, the antiparallel merging model predicts the frequent occurrence of equatorward moving events.

In contrast to the merging models, the pressure pulse model does not predict that event occurrence or orientation depend upon the IMF orientation. Pressure pulse driven ripples move radially outward from a point on the magnetopause where solar wind discontinuities make first contact. This point lies prior to local noon during rare periods of orthospiral IMF orientation and after local noon during the more common intervals of spiral IMF orientation. Sunward moving events can be expected just prior to local noon during periods of orthospiral IMF and just after local noon during periods of spiral IMF. Events should generally move poleward away from the initial (equatorial) point of contact.

We identified 59 transient events in the CCE data set on the basis of magnetic field strength increases and bipolar signatures normal to the nominal magnetopause. Using the bipolar signatures normal to the nominal magnetopause, we determined that most events move poleward. Our results are consistent with the near-equatorial source for transient events inferred by previous studies. We then used minimum variance analysis to demonstrate that most events in our data set are closely aligned with the geomagnetic equator, consistent with extended two-dimensional events originating in the equatorial region.

A comparison with simultaneous solar wind observations indicated that neither the IMF  $B_y$ , nor  $B_z$  components has any significant effect upon magnetospheric event occurrence or orientation. Finally, we showed that only about half of the sunward moving events moved in the direction predicted by magnetic curvature forces. On these grounds, we ruled out bursty merging as the predominant cause of the transient events in our study.

On the other hand, the lack of any clear IMF dependence upon event occurrence and orientation were consistent with the predictions of the pressure pulse model. Furthermore, we showed that most of the sunward moving events observed after local noon occurred during intervals of spiral IMF orientation, whereas most of the sunward moving events observed prior to local noon occurred during intervals of orthospiral IMF orientation. We concluded that these observations were consistent with an interpretation of pressure pulses as the dominant cause of the transient events in our study.

Our identification of pressure pulses as the dominant cause of transient events in the dayside magnetosphere agrees with that reached by other authors who used CCE and geosynchronous observations, but disagrees with the results of studies which made use of observations in the immediate vicinity of the magnetopause. The latter studies showed that event occurrence and characteristics depend profoundly on the IMF orientation, consistent with an interpretation in terms of bursty merging.

We tried to reconcile the conflicting results with an interpretation invoking two parallel mechanisms for generating transient events. We argued that bursty merging at the magnetopause might produce many small amplitude perturbations to the magnetospheric magnetic field, whereas pressure pulses produce a few large amplitude events. Satellites in the vicinity of the magnetopause would observe all the events, resulting in a data

base dominated by bursty merging events. Satellites deep within the magnetosphere would observe only those events with the largest amplitudes, resulting in a database dominated by pressure-pulse events.

Thus, the observations and interpretation presented in this study do not rule out the occurrence of transient events produced by bursty merging at the magnetopause. They do, however, indicate that such events produce signatures deeper within the magnetosphere which are negligible in comparison with those generated by pressure-pulse driven ripples on the magnetopause.

**Acknowledgments.** We thank T. A. Potemra and the AMPTE CCE data center for supplying the CCE magnetometer observations, and the NSSDC for supplying the GSFC IMP 8, ISEE 2, and AMPTE IRM magnetometer observations. Work at LMU was supported by the NASA/JOVE program. Work at APL was supported by NASA under Task 1 of Space and Naval Warfare Systems Command contract N00039-91-C-5001 to the Navy.

The Editor thanks G. Paschmann and S. W. H. Cowley for their assistance in evaluating this paper.

## References

- Baumjohann, W., and G. Paschmann, Solar wind-magnetosphere coupling: Processes and observations, *Phys. Scr.*, **T18**, 61–72, 1987.
- Berchem, J., and C. T. Russell, The thickness of the magnetopause current layer: ISEE 1 and 2 observations, *J. Geophys. Res.*, **87**, 2108–2114, 1982.
- Berchem, J., and C. T. Russell, Flux transfer events on the magnetopause: Spatial distribution and controlling factors, *J. Geophys. Res.*, **89**, 6689–6703, 1984.
- Borodkova, N., G. Zastenker, and D. G. Sibeck, A case and statistical study of transient events at geosynchronous orbit and their solar wind origin, *J. Geophys. Res.*, **100**, 5643–5656, 1995.
- Bryant, D. A., S. M. Krimigis, and G. Haerendel, Outline of the Active Magnetospheric Particle Tracer Explorers (AMPTE) mission, *IEEE Trans. Geosci. Remote Sens.*, **GE-23**, 177–181, 1985.
- Cowley, S. W. H., Comments on the merging of nonantiparallel magnetic fields, *J. Geophys. Res.*, **81**, 3455–3458, 1976.
- Cowley, S. W. H., The causes of convection in the Earth's magnetosphere: A review of developments during the IMS, *Rev. Geophys.*, **20**, 531–565, 1982.
- Cowley, S. W. H., and C. J. Owen, A simple illustrative model of open flux tube motion over the dayside magnetopause, *Planet. Space Sci.*, **37**, 1461–1475, 1989.
- Crooker, N. U., Dayside merging and cusp geometry, *J. Geophys. Res.*, **84**, 951–959, 1979.
- Daly, P. W., M. A. Saunders, R. P. Rijnbeek, N. Scokpe, and C. T. Russell, The distribution of reconnection geometry in flux transfer events using energetic ion, plasma and magnetic data, *J. Geophys. Res.*, **89**, 3843–3854, 1984.
- Elphic, R. C., and D. J. Southwood, Simultaneous measurements of the magnetopause and flux transfer events at widely separated sites by AMPTE UKS and ISEE 1 and 2, *J. Geophys. Res.*, **92**, 13666–13672, 1987.
- Fairfield, D. H., Average and unusual locations of the Earth's magnetopause and bow shock, *J. Geophys. Res.*, **76**, 6700–6716, 1971.
- Farrugia, C. J., R. C. Elphic, D. J. Southwood, and S. W. H. Cowley, Field and flow perturbations outside the reconnected field line region in flux transfer events: Theory, *Planet. Space Sci.*, **35**, 227–240, 1987.
- Gonzalez, W. D., and F. S. Mozer, A quantitative model for the potential resulting from reconnection with an arbitrary interplanetary magnetic field, *J. Geophys. Res.*, **79**, 2520–2528, 1974.
- Hassam, A. B., Transmission of Alfvén waves through the Earth's bow shock: Theory and observation, *J. Geophys. Res.*, **83**, 643–653, 1978.
- Huba, J. D., N. T. Gladd, and K. Papadopoulos, The lower-hybrid-drift instability as a source of anomalous resistivity for magnetic field line reconnection, *Geophys. Res. Lett.*, **4**, 125–128, 1977.
- Kawano, H., S. Kokubun, and K. Takahashi, Survey of transient magnetic field events in the dayside magnetosphere, *J. Geophys. Res.*, **97**, 10677–10692, 1992.
- King, J. H., Availability of the IMP 7 and IMP 8 data for the IMS period, in *The IMS Source Book*, edited by C. T. Russell and D. J. Southwood, pp. 10–20, AGU, Washington, D. C., 1982.
- Korotova, G. I., and D. G. Sibeck, A case study of transient event motion in the magnetosphere and in the ionosphere, *J. Geophys. Res.*, **100**, 35–46, 1995.
- Kuo, H., C. T. Russell, and G. Le, Statistical studies of flux transfer events, *J. Geophys. Res.*, **100**, 3513–3519, 1995.
- Lanzerotti, L. J., Comment on "Solar wind dynamic pressure variations and transient magnetospheric signatures," *Geophys. Res. Lett.*, **16**, 1197–1199, 1989.
- Lemaire, J., Impulsive penetration of filamentary plasma elements into the magnetospheres of the Earth and Jupiter, *Planet. Space Sci.*, **25**, 887–890, 1977.
- Lockwood, M., M. F. Smith, C. J. Farrugia, and G. L. Siscoe, Ionospheric ion upwelling in the wake of flux transfer events at the dayside magnetopause, *J. Geophys. Res.*, **93**, 5641–5654, 1988.
- Luhmann, J. G., R. J. Walker, C. T. Russell, N. U. Crooker, J. R. Spreiter, and S. S. Stahara, Patterns of potential magnetic field merging sites on the dayside magnetopause, *J. Geophys. Res.*, **89**, 1739–1742, 1984.
- Lühr, H., N. Klöcker, W. Oehlschlägel, B. Häusler, and M. Acuña, The IRM fluxgate magnetometer, *IEEE Trans. Geosci. Remote Sens.*, **GE-23**, 259–261, 1985.
- Lui, A. T. Y., C.-L. Chang, A. Mankofsky, H.-K. Wong, and D. Winske, A cross-field current instability for substorm expansions, *J. Geophys. Res.*, **96**, 11389–11401, 1991.
- Papamastorakis, I., G. Paschmann, W. Baumjohann, B. U. Ö. Sonnerup, and H. Lühr, Orientation, motion, and other properties of flux transfer event structures on September 4, 1984, *J. Geophys. Res.*, **94**, 8852–8866, 1989.
- Potemra, T. A., L. J. Zanetti, and M. H. Acuna, The AMPTE CCE magnetic field experiment, *IEEE Trans. Geosci. Remote Sens.*, **GE-23**, 246–249, 1985.
- Rijnbeek, R. P., S. W. H. Cowley, D. J. Southwood, and C. T. Russell, A survey of dayside flux transfer events observed by the ISEE 1 and 2 magnetometers, *J. Geophys. Res.*, **89**, 786–800, 1984.
- Russell, C. T., and R. C. Elphic, Initial ISEE magnetometer results: Magnetopause observations, *Space Sci. Rev.*, **22**, 681–715, 1978.
- Russell, C. T., J. Berchem, and J. G. Luhmann, On the source region of flux transfer events, *Adv. Space Res.*, **5**, 363–368, 1985.
- Schindler, K., A theory of the substorm mechanism, *J. Geophys. Res.*, **79**, 2803–2810, 1974.
- Sibeck, D. G., A model for the transient magnetospheric response to sudden solar wind dynamic pressure variations, *J. Geophys. Res.*, **95**, 3755–3771, 1990.
- Sibeck, D. G., Transient events in the outer magnetosphere: Boundary waves or flux transfer events?, *J. Geophys. Res.*, **97**, 4009–4026, 1992.
- Sibeck, D. G., Transient and quasi-periodic (5–15 min) events in the outer magnetosphere, in *Solar Wind Sources of Magnetospheric Ultra-Low-Frequency Waves*, *Geophys. Monogr. Ser.*, vol. 81, edited by M. J. Engebretson, K. Takahashi, and M. Scholer, pp. 173–182, AGU, Washington, D. C., 1994.
- Sibeck, D. G., and P. T. Newell, IMF orientation for transient events in the outer magnetosphere, *J. Geophys. Res.*, **100**, 175–183, 1995.
- Sibeck, D. G., W. Baumjohann, R. C. Elphic, D. H. Fairfield, J. F. Fennel, W. B. Gail, L. J. Lanzerotti, R. E. Lopez, H. Lühr, A. T. Y. Lui, C. G. MacLennan, R. W. McEntire, T. A. Potemra, T. J. Rosenberg, and K. Takahashi, The magnetospheric response to 8-min-period strong-amplitude upstream pressure variations, *J. Geophys. Res.*, **94**, 2505–2519, 1989a.
- Sibeck, D. G., W. Baumjohann, and R. E. Lopez, Reply, *Geophys. Res. Lett.*, **16**, 1200–1202, 1989b.
- Siscoe, G. L., L. Davis, Jr., P. J. Coleman Jr., E. J. Smith, and D. E. Jones, Power spectra and discontinuities of the interplanetary magnetic field: Mariner 4, *J. Geophys. Res.*, **73**, 61–82, 1968.
- Sonnerup, B. U. Ö., Magnetopause reconnection rate, *J. Geophys. Res.*, **79**, 1546–1549, 1974.
- Sonnerup, B. U. Ö. and L. J. Cahill, Jr., Magnetopause structure and attitude from Explorer 12 observations, *J. Geophys. Res.*, **72**, 171–183, 1967.
- Southwood, D. J., Magnetopause Kelvin-Helmholtz instability, in *Magnetospheric Boundary Layers*, edited by B. Battrick, *Eur. Space Agency Spec. Publ.*, **SP-148**, 357–364, 1979.
- Southwood, D. J., M. A. Saunders, M. W. Dunlop, W. A. C. Mier-Jedrzejowicz, and R. P. Rijnbeek, A survey of flux transfer events

- recorded by the UKS spacecraft magnetometer, *Planet. Space Sci.*, **34**, 1349–1359, 1986.
- Southwood, D. J., C. J. Farrugia, and M. A. Saunders, What are flux transfer events?, *Planet. Space Sci.*, **36**, 503–508, 1988.
- Völk, H. J., and R. D. Auer, Motions of the bow shock induced by interplanetary disturbances, *J. Geophys. Res.*, **79**, 40–48, 1974.
- Walthour, D. W., B. U. Ö. Sonnerup, G. Paschmann, H. Lüher, D. Klumpar, and T. Potemra, Remote sensing of two-dimensional magnetopause structures, *J. Geophys. Res.*, **98**, 1489–1504, 1993.
- Wu, B. H., M. E. Mandt, L. C. Lee, and J. K. Chao, Magnetospheric response to solar wind dynamic pressure variations: Interaction of interplanetary tangential discontinuities with the bow shock, *J. Geophys. Res.*, **98**, 21297–21311, 1993.
- 
- C. T. Russell, Institute for Geophysics and Planetary Physics, University of California, Los Angeles, CA 90024.
- J. Sanny and C. C. Venturini, Physics Department, Loyola Marymount University, Los Angeles, CA 90045.
- D. G. Sibeck, Applied Physics Laboratory, Johns Hopkins University, Johns Hopkins Road, Laurel, MD 20723-6099. (e-mail: david.sibeck@jhuapl.edu)

(Received June 2, 1995; revised September 7, 1995; accepted October 4, 1995.)